Pergamon

Int. J. Hydrogen Energy Vol. 21, No. 6, pp. 479–484, 1996

0360-3199/96 $15.00 + 0.00

0360-3199(95)00111-5

THE HYDRIDING KINETICS OF $MlNi_5$—II. EXPERIMENTAL RESULTS

X. H. WANG, C. S. WANG, C. P. CHEN, Y. Q. LEI and Q. D. WANG

Department of Materials Science and Engineering, Zhejiang University, Hang Zhou, 310027, P. R. China

(*Received for publication* 27 *September* 1995)

Abstract—The hydriding kinetics of $MlNi_5$ before and after activation were studied experimentally and discussed in terms of the models presented in Part I. The parameters in the kinetic equations previously obtained were determined. The experimental data were in excellent agreement with the equations. The results indicate that the first hydrogenation process is a phase transformation process, in which the nucleation and growth of β-phase is the hydriding rate-controlling step. After activation, the hydriding process is governed by a mixed-controlled mechanism, with the hydriding controlling step varying with the applied pressure and transformed fraction. Copyright © 1996 International Association for Hydrogen Energy

NOMENCLATURE

$C_{\beta\alpha}$, $C_{\alpha\beta}$	The hydrogen concentration of the β- or α-hydride equilibriating with P_{eq} at the interface between the α- and the β-phase
D_α, D_β	Diffusion coefficient of hydrogen atoms in α- and β-phase
P_a	Nucleation barrier
K_1, K_2	Reaction rate constants
K_0	Ratio of active areas to the total area of the sample surface
K_t	Constant, representing the constraint in the hydrogen activity
K_s	Rate constant for hydrogen transition from the surface to the matrix
K_R	$\dfrac{\sqrt{K_1}}{\sqrt{K_2}+\sqrt{K_1 P_{H_2,i}}}$
K'	Constant$\left(=\dfrac{C_{\alpha\beta}}{C_{\beta\alpha}}\right)$
K'_0	Coefficient
m	Number of particles
N_0	Number of sites in unit volume
n'	Constant, depending on the nucleation rate, the growth rate and the shape of the hydride
P'_{eq}, P_{eq}	Equilibrium pressure for the first hydrogenation and after activation
$P_{H_2,i}$	Hydrogen pressure at the outside of sample
P_0, P_{H_2}	Applied hydrogen pressure
r_0	Radius of the material particle
t	Reaction time
X	Ratio of hydrogen concentration at any time to saturate hydrogen concentration equilibrating with P_0
X_β	β-phase transformed fraction
$\dfrac{dn}{dt}$, $\dfrac{dX}{dt}$, $\dfrac{dX_\beta}{dt}$	The hydriding rate

1. INTRODUCTION

In the previous paper (hereafter denoted as Part I [1], a reaction kinetic model for the hydriding reaction of hydrogen storage alloy was proposed, in which the hydriding process was divided into three steps. Kinetic equations for the cases when each of the three steps is the rate-controlling step, respectively, have been derived.

In this work, we studied the hydriding kinetics of $MlNi_5$ at 30°C and in the hydrogen pressure range of 1.05–3.0 MPa, and obtained values for the parameters of the kinetic equations. The dependence of the hydriding rate on the transformed fraction and the variation of hydriding rate with the applied hydrogen pressure were determined experimentally and compared with the kinetic equation curves. It was found that the test results fitted these equations very well. From these results, we believe that the nucleation and growth of the β-phase is the rate-controlling step for the first hydrogenation process, while after activation, the hydriding process is governed by a mixed-controlled mechanism.

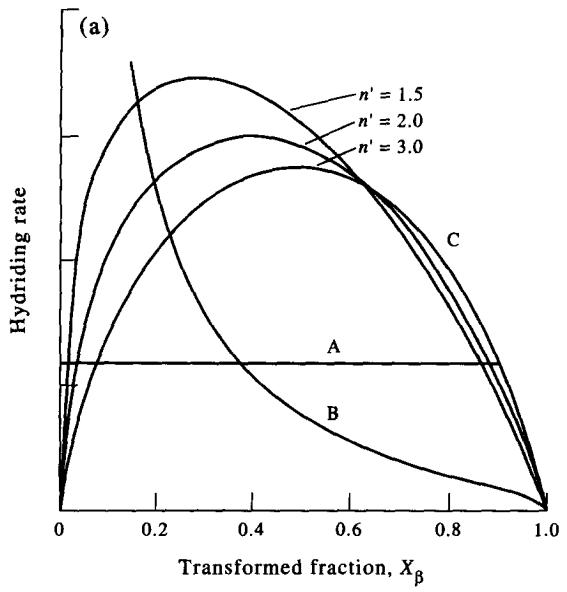

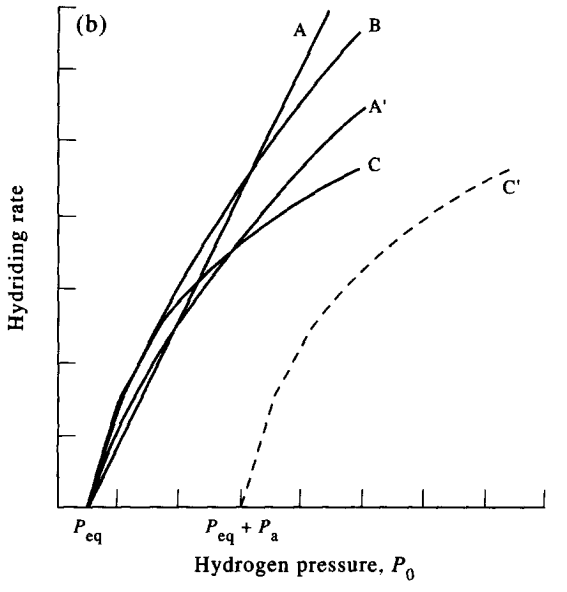

Fig. 1. (a) Schematic diagram of hydriding rate versus transformed fraction X_β and (b) schematic diagram of hydriding versus applied hydrogen pressure.

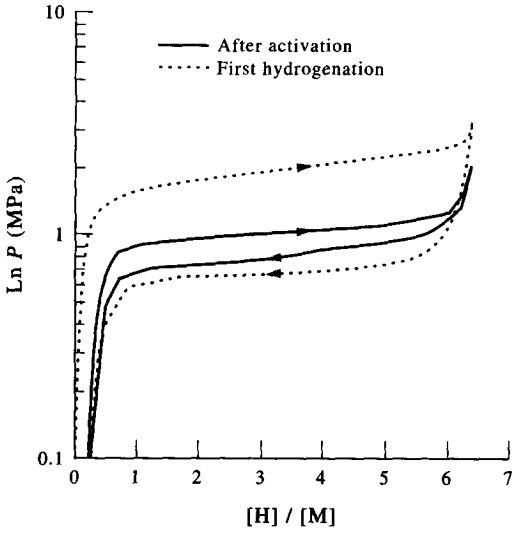

Fig. 2. The P–C–T curves for $MlNi_5$–H system at 30°C.

2. THE KINETIC MODEL AND KINETIC EQUATIONS

As stated in our kinetic model of Part I, the hydriding process is believed to be divided into three steps: (i) the dissolution of hydrogen in the alloy (or its hydride); (ii) hydrogen diffusion through the alloy (or its hydride); (iii) phase transformation (β-hydride depositing from supersaturated α-solid solution). The hydrogen dissolution can be further divided into dissociative chemisorption and boundary transition. Kinetic equations are derived for each one of the three steps as the rate controlling step, as follows:

(1) When the dissolution of hydrogen into hydride is the rate controlling step

$$\text{(at lower } P_0) \quad \frac{dX_\beta}{dt} = \frac{3K_R K_2}{r_0 K_1 \sqrt{P_{eq}}}(P_0 - P_{eq}) \tag{1}$$

$$\text{(at higher } P_0) \quad \frac{dX_\beta}{dt} = \frac{3K_s}{r_0}\left(\sqrt{\frac{P_0}{P_{eq}}} - 1\right) \tag{2}$$

(2) When the diffusion of hydrogen atoms is the rate-controlling ste

$$\frac{dX_\beta}{dt} = 3D_\beta\left(\sqrt{\frac{P_0}{P_{eq}}} - 1\right)/\{r_0^2[(1 - X_\beta)^{-1/3} - 1](1 - K')\} \tag{3}$$

(3) When the phase transformation (nucleation and growth of the β-phase) is the rate controlling step

$$\frac{dX_\beta}{dt} = n'K_0'(1 - X_\beta)[-\mathrm{Ln}(1 - X_\beta)]^{\frac{n'-1}{n'}} \mathrm{Ln}\frac{P_0 - P_a}{P_{eq}} \tag{4}$$

as the activation proceeds, P_a decreases and becomes close to zero after activation. Figures 1a and b are the schematic diagrams for the hydriding rate versus transformed fraction X_β and applied hydrogen pressure, respectively.

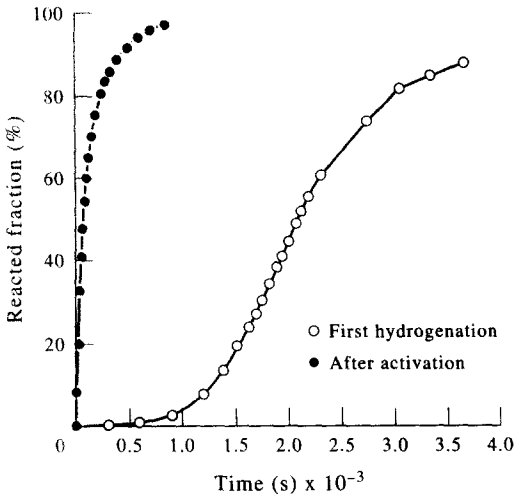

Fig. 3. The activation kinetic curves of $MlNi_5$ at 30°C and 3.0 MPa.

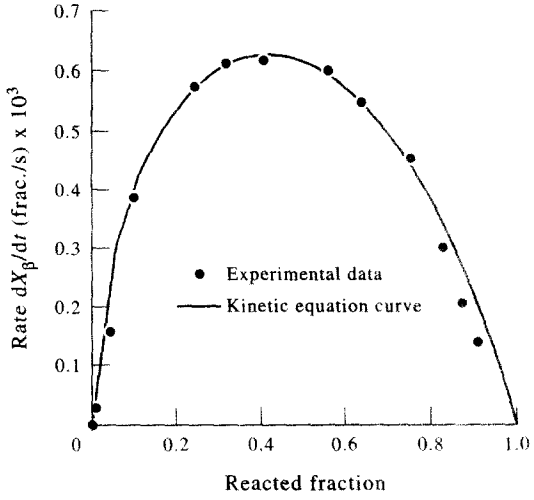

Fig. 4. The dependence of hydriding rate on reacted fraction of $MlNi_5$.

3. EXPERIMENTAL

The contents and purities of the raw materials used in the experiment are as follows: La-rich mischmetal (Ml) 43.9% La, 5.1% Ce, 11% Pr, 38% Nd, and 2% other rare earths, metallic nickel of 99.9% purity, and 99.999% hydrogen. The samples were prepared by arc melting under an argon atmosphere and remelted more than twice to assure good homogeneity. The prepared samples were inspected with X-ray diffraction and were found to be single phased with $CaCu_5$ structure. Chemical analysis also showed that the compositions of the samples were close to the stoichiometric values. The particle size measured by SEM was about 5–15 μm.

Each sample was crushed to about 100 mesh in air and then loaded into a copper reactor. The amount of sample was about 1 g to reduce the effect of hydriding heat. The temperature was accurately controlled using a large water bath. The first hydrogenation process was measured by means of the volumetric method. After more than 20 hydriding and dehydriding cycles, the hydriding kinetics were measured by using the pressure sweep method, which was similar to that of Lee [2], with the amount of hydrogen absorbed measured with a pressure tranducer by monitoring the pressure drop of hydrogen in the reacted system. The output of the pressure transducer was connected to a dynamic strain gauge and recorded by an x–y recorder. The measurement of P–C–T plots has been described elsewhere [3].

4. DETERMINATION OF PARAMETERS

4.1. *Determination of parameters*

The particle size observed by SEM is about 5–15 μm, in the kinetic equation, the radius of the particles (r_0) is taken as an average value of 5 μm. The hydrogen diffusion coefficients in $LaNi_5$ and $MmNi_5$ and their multicomponent alloys are in the range of 10^{-8}–10^{-11} cm^2 s^{-1} [4], in the $MlNi_5$ alloy, we take D_β roughly as 7.5×10^{-10} cm^2 s^{-1}. The hydriding equilibrium pressures for the first hydrogenation and after activation are $P'_{eq} = 1.9$ MPa and $P_{eq} = 1$ MPa, respectively, and the constant $K'(=C_{\alpha\beta}/C_{\beta\alpha}) = 0.124$ as shown in Fig. 2.

4.2. *Determination of activation kinetic equation*

The test results indicate that $MlNi_5$ has a large hydrogen storage capacity as shown in Fig. 2. It can be activated easily under 3.0 MPa hydrogen pressure at 30°C. Figure 3 shows its activation kinetic curves, the incubation period is less than 10 min. The experimental data of the dependence of the hydrogen absorption rate on the reacted fraction are presented in Fig. 4 (full circles). Comparing the test results with the curves in Fig. 1, we believe that the hydriding reaction of $MlNi_5$ for the first hydrogenation process is characteristic of that of phase transformation (nucleation and growth mechanism). From the experimental data in Fig. 4, the parameters of the first hydrogenation process in equation (4) are determined as

$$n' = 2.1$$

$$K'_0 = 9.558 \times 10^{-4}\ (s^{-1})$$

$$P_a = 0.9\ \text{MPa}$$

The kinetic equation for the first hydrogenation process is

$$\frac{dX_\beta}{dt} = 0.001489 \times (1 - X_\beta) \times [-\text{Ln}(1 - X_\beta)]^{0.5238}\ \text{Ln}(p_0 - 0.9) \quad (5)$$

The test results are in excellent agreement with the kinetic equation curve. From Figs 3 and 4, it is clear that the

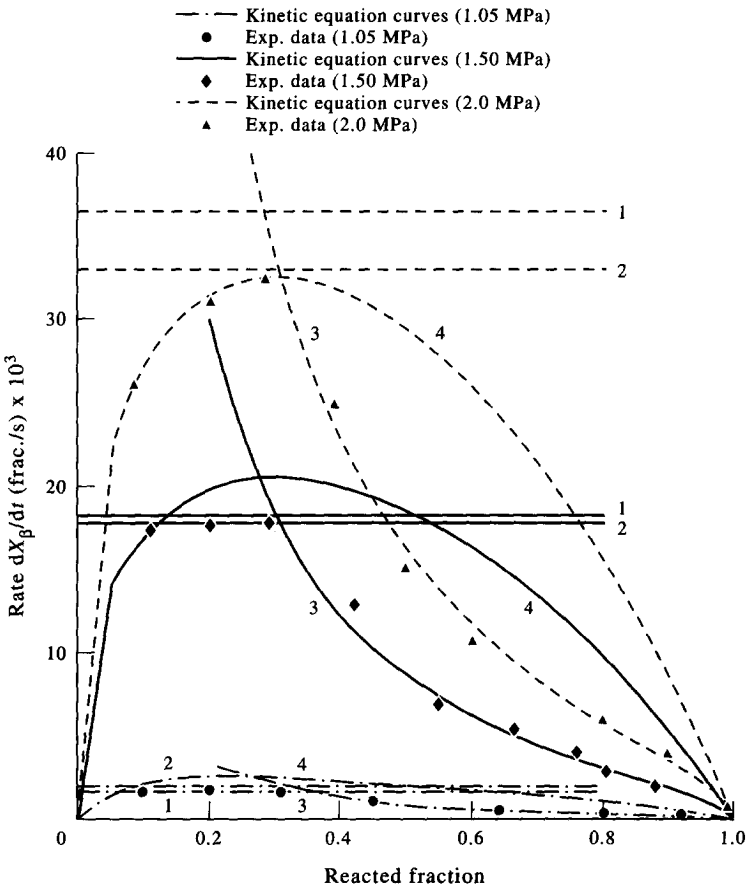

Fig. 5. The variation of hydriding rate with the transformed fraction at 30°C and various applied pressures. 1. Dissociative chemisorption (equation (6)) 2. Boundary transition (equation (7)) 3. Hydrogen diffusion (equation (8)) 4. Nucleation and growth (equation (9)).

first hydrogenation process of $MlNi_5$ is a phase transformation process, the hydriding rate is governed by nucleation and growth of the β-phase.

After activation, the variation of the hydriding rate of $MlNi_5$ with the transformed fraction and various hydrogen pressure are shown in Fig. 5. When the applied hydrogen pressure is small, the hydrogen absorption rate is constant at first and unchanged with the transformed reaction at the initial stage of the hydriding process, but decreased with the transformed reaction at the later stage (circles in figure). As the applied hydrogen pressure increases, the hydrogen absorption rate is not constant any more. The hydriding rate increases up to a maximum value and then decreases (full triangle).

With the test results compared with the curves in Fig. 1, we believe that at lower applied hydrogen pressure, the hydriding controlling step changes from hydrogen dissolution at the initial stage to hydrogen diffusion at the later stage, while at high hydrogen pressure, the controlling step changes from nucleation and growth of the β-phase to hydrogen diffusion. Fitting the test result to equations (1)–(4), we obtain the values of the parameters of hydrogenation after activation as follows:

$$P_a = 0$$

$$n' = 1.55,$$

$$K_0' = 6.25 \times 10^{-2}\ (s^{-1})$$

$$K = K_R K_2 / K_1 = 6.08 \times 10^{-6}\ (\text{cm MPa}^{-1/2}\ s^{-1})$$

$$K_s = 1.327 \times 10^{-5}\ (\text{cm MPa}^{-1/2}\ s^{-1}).$$

By substituting the above parameters into equations (1)–(4), we obtain the kinetic equations for the hydriding process after activation as follows. For hydrogen-dissolution-rate-controlled kinetic equations

$$\text{(at lower } P_0) \qquad \frac{dX_\beta}{dt} = 0.03648 \times (P_0 - 1) \tag{6}$$

$$\text{(at higher } P_0) \qquad \frac{dX_\beta}{dt} = 0.09762 \times (\sqrt{P_0} - 1). \tag{7}$$

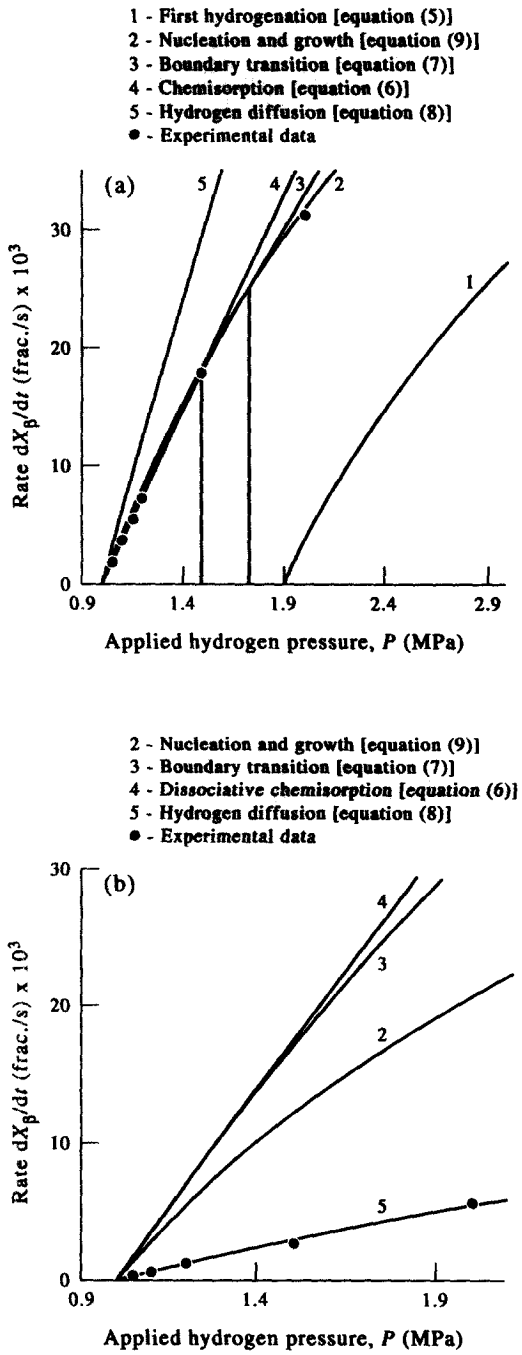

Fig. 6. The hydriding rate versus the applied hydrogen pressure (a) $X_\beta = 0.2$; (b) $X_\beta = 0.8$.

For hydrogen-diffusion-rate-controlled kinetic equation

$$\frac{dX_\beta}{dt} = 0.01029 \times (\sqrt{P_0} - 1)/\{r_0^2[(1 - X_\beta)^{-1/3} - 1]\}. \quad (8)$$

For nucleation and growth of the β-phase limited kinetic equation

$$\frac{dX_\beta}{dt} = 0.09688 \times (1 - X_\beta)[-\mathrm{Ln}(1 - X_\beta)]^{0.3548}\ \mathrm{Ln}(p_0). \quad (9)$$

5. EXPERIMENTAL RESULTS AND DISCUSSION

5.1. *The hydriding kinetics of* $MlNi_5$ *at constant pressure*

The kinetic curves based on equations (6)–(9) for $P = 1.05$, 1.5 and 2.0 MPa are also plotted in Fig. 5. From this figure, it can be seen that the test results agree with the rule that the step with the lowest rate governs the hydriding process. The straight lines 1 and 2 are for the cases when the hydriding rate controlling steps are dissociative chemisorption and boundary transition, respectively, curve 3 is for the case when the hydriding process is governed by hydrogen diffusion through the hydride phase, and curve 4 is for the case when nucleation and growth is the hydriding rate controlling step. When the applied hydrogen pressure is small, the level of line 1 is lower than that of line 2, and when the reacted fraction is large, the hydrogen-diffusion-rate-limited hydriding kinetic equation curve becomes the lowest one. The experimental data fit line 1 and curve 3 very well. This means that, for this case, the hydriding mechanism changes from the hydrogen-dissociative-chemisorption-rate-limited mechanism at the initial hydriding stage (except for the considerably small reacted fraction) to the hydrogen-diffusion-limited one at the later stage. As the applied hydrogen pressure increases, the level of line 1 becomes higher than that of line 2, which it means that the hydriding rate controlling step changes from hydrogen dissociative chemisorption to boundary transition when the reacted fraction is small. When the applied hydrogen pressure is high, the hydrogen is dissolved into the sample (both dissociative chemisorption and boundary transition) rather quickly; the hydriding rate is governed by nucleation and growth and the hydrogen diffusion mechanism. As the hydrogenation proceeds, the hydriding rate controlling step changes from nucleation and growth of the β-phase to hydrogen diffusion.

5.2. *The hydriding kinetics of* $MlNi_5$ *at definite transformed fraction*

The dependence of the hydriding rate on the applied hydrogen pressure is presented in Fig. 6a and b for the reacted fractions 0.2 and 0.8, respectively.

As previously stated, the first hydrogenation is a process of nucleation and growth of the β-phase as shown in Fig. 6a curve 1, because even a few defects in the matrix make the nucleation and growth of the β-phase very difficult, its nucleation barrier is $P_a = 0.9$ MPa (see Section 4.2). As the hydriding/dehydriding cycle proceeds, P_a decreases and becomes zero after activation. This means that curve 1 will move in a parallel manner towards the low pressure side and finally coincide with curve 2.

It is due to this fact that the defects caused by the volume expansion of hydrogenation make nucleation and growth of the β-phase fast and easy. From Fig. 6a, we can also see that, when the reacted fraction is small ($X_\beta = 0.2$), at a low applied hydrogen pressure 0.1 MPa $< p <$ 1.72 Pa as shown in Fig. 6a, the dissolution of hydrogen is the rate controlling step. At first, at $p < 1.5$ MPa the dissociative chemisorption controls the dissolution, but at 1.5 MPa $< p <$ 1.72 MPa (see Fig. 6a), the rate controlling step of dissolution changes from dissociative chemisorption to boundary transition, the relation of the hydriding rate to applied pressure also changes from being proportional to p to proportional to $p^{1/2}$. As the applied hydrogen pressure increases further, i.e. $p > 1.72$ MPa, the dissolution rate will be much faster and easier. Then, the rate controlling step will change from the boundary transition to nucleation and growth. Figure 6b indicates that at the final hydriding stage, hydrogen diffusion through the hydride phase controls the hydriding process. As the hydriding continues, the rate of diffusion becomes slower. Hence in the $\alpha + \beta$ two-phase coexisting region, the β-phase starts to form a continuous layer which grows gradually. When the width of the hydride becomes thick, the diffusion distance will be longer. This makes the hydrogen diffusion through the hydride phase the rate-controlling step.

From Figs 5 and 6, we believe that the hydriding process of $MlNi_5$ after activation is governed by a mixed controlled mechanism, and not by any one mechanism, the hydriding rate controlling step changes with the reacted fraction and the applied hydrogen pressure. At low applied hydrogen pressure, the hydriding rate-controlling step changes from hydrogen dissolution to hydrogen diffusion, while at high applied hydrogen pressure, the hydriding rate-controlling step changes from nucleation and growth to hydrogen diffusion.

6. CONCLUSION

(1) The first hydrogenation process of $MlNi_5$ is a phase transformation process, the rate-controlling step is nucleation and growth of the β-phase because there exist fewer defects in the matrix, and its kinetics can be described satisfactorily by the JMA equation.

(2) After activation, when the applied hydrogen pressure is low, the rate controlling step in the hydriding process of $MlNi_5$ is the dissociative chemisorption of hydrogen molecules on the $MlNi_5$ surface. With the increasing applied hydrogen pressure which makes the dissociative chemisorption faster, the boundary transition becomes the controlling step. In this stage, the hydriding rate is controlled by dissolution of hydrogen. As the applied pressure increases further, the nucleation and growth of the hydride control the hydriding rate. In the later stage, regardless of the applied hydrogen pressure, hydrogen diffusion through the hydride phase is the rate-controlling step.

REFERENCES

1. C. S. Wang, X. H. Wang, Y. Q. Lei and Q. D. Wang, *Int. J. Hydrogen Energy* **21**(6), 471 (1996).
2. C. N. Park and J. Y. Lee, *J. less-common Metals* **91**, 189 (1983).
3. X. H. Wang, C. P. Chen, M. Yan, J. Wu and Q. D. Wang, *J. Rare Earths* **12**(3) (1994).
4. J. S. Hang, Z. X. Zhou, F. Y. Yao *et al.*, *Battery Bimonthly* (in Chinese) **2**, 69 (1994).